Modeling Monomer Transport by Convection during Olefin Polymerization

U. Parasu Veera and G. Weickert
Dutch Polymer Institute/Dept. of Chemical Technology, University of Twente, 7500 AE Enschede, The Netherlands

U. S. Agarwal
Dutch Polymer Institute/Dept. of Chemical Technology, Eindhoven University of Technology, 5600 MB Eindhoven, The Netherlands

During olefin polymerization on heterogeneous catalyst, a catalyst particle undergoes fragmentation, and the formed polymer gets deposited on the fragments. These polymer-coated fragments (microparticles) together form a porous polymer particle (macroparticle). The multigrain model (MGM) gives a detailed description by accounting for the monomer diffusion phenomena at both levels. The original approach to solution involved a sequential shell-by-shell determination of monomer concentration profiles, with both radial boundaries of the shells moving with the particle growth. A fixed boundary system of simultaneous differential equations enables easier computer implementation of the MGM model. Further, in a new development presented here, the interstitial spaces between the microparticles make up the pores through which monomer transport occurs not only by diffusion, but also by convection. The convection is driven by the pressure gradient created by the monomer consumption within the particle. Consistent with recent experimental observations, significantly higher monomer transport rates are thus predicted.

Introduction

Diffusional limitation during heterogeneously catalyzed olefin polymerization has been modeled in the form of the polymeric flow model (PFM) (Singh and Merrill, 1971; Schmeal and Street, 1971; Galvan and Tirrell, 1986) and later more extensively as the multigrain model (MGM) (Yermakov et al., 1970; Nagel et al., 1986; Floyd et al., 1987; Hutchinson et al., 1992). The PFM offers the advantage of relative mathematical simplicity, particularly since the moving-boundary problem is easily transformed into a fixed-boundary problem, thereby facilitating easy numerical solution. The MGM incorporates a more detailed picture of the underlying phenomena on the microparticle and the macroparticle scales at the cost of increased numerical complexity. We begin by showing that the physical details of the simple MGM can in fact be incorporated easily in the PFM, while retaining the ease of numerical simulation of the fixed-boundary adaptation of the PFM (Galvan and Tirrell, 1986). Then, we proceed to incorporate in this model an additional mode of monomer transport into the polymer particle, that is, monomer convection through the interconnected *pores* in the two-phase particle.

During olefin polymerization on heterogeneous catalyst, the catalyst particle undergoes fragmentation and the polymer so formed gets deposited on the fragments. These polymer-coated fragments (microparticles) together form a porous polymer particle (macroparticle). The overall reaction rate can be limited by the monomer transport, first through the porous macroparticle, and then within the microparticle (to the active sites on the catalyst fragments). The PFM, first proposed by Schmeal and Street (1971) and Singh and Merrill (1971), provides a simple description of the phenomena. It assumes the intraparticle mass transfer to be simply Fickian diffusion through the polymer. Galvan and Tirrell (1986) considered a mathematical transformation to convert the moving-boundary problem into a fixed-boundary problem.

Correspondence concerning this article should be addressed to U. S. Agarwal.

They concluded that polydispersities higher than 2 can result from diffusional limitations only at Thiele modulus [$\alpha = \sqrt{R_o^2(k_p/D)A_o}$] values greater than $\sqrt{10}$. Hence, they attributed the observed high polydispersity at the smaller α primarily to multiple active sites. A crucial correction to their mathematical transformation was presented many years later by Byrne (1993). This was used by Hoel et al. (1994) to attribute the observed copolymer composition variation in the polymer particle to the monomer diffusional limitations.

The MGM more directly takes into account the heterogeneous nature of the growing polymer particle. The growth of the microparticle by the polymer deposition around the catalyst fragment, and the growth of the macroparticle (agglomerate of the microparticles) is explicitly considered. A dimensional analysis of the relevant parameter values to determine presence of diffusional resistance was presented by Floyd et al. (1986). Considering peak polymerization rates of 5,000 g/g-cat h, Floyd et al. (1987) concluded that significant diffusional resistance only occurs if the macroparticle level diffusivity is 10^{-5} cm^2/s or lower. They also concluded that for macroparticle diffusivity of 2×10^{-6} cm^2/s for slurry-phase olefin polymerization, reaction rates in excess of 20,000 g/g-cat h could not be predicted without wastefully using excess active metal. Hutchinson et al. (1992) predicted diffusional limitations during the first hour of slurry-phase polymerization at the rate of 2000–10,000 g/g-cat h. McKenna et al. (1997) and Weickert et al. (1999) have shown that the peak high activities observed with the modern catalyst cannot be explained by the Fickian diffusion of monomers. There has been much effort to experimentally examine if the monomer transport limitations do exist. However, a conclusion has been elusive, as the observable effects, such as slowing polymerization rate, higher polydispersity, and particle-size dependence, can also result from chemical deactivation of sites, existence of multiple active sites, and nonuniformity of catalyst loading, respectively (see Agarwal, 1998; Przybyla et al., 1999a).

The alternative mode of monomer transport in the polymer particle is the monomer convection through the pores, driven by the pressure drop caused by the monomer consumption by the reaction. Although this has been recognized to be the dominant mechanism during homopolymerization in the absence of diluents (Floyd et al., 1986; Weickert et al., 1999), it has not been incorporated in the mathematical formulations (Naik and Ray, 2001). Yet in situations involving catalysts of not so high activity, a Fickian diffusion mechanism (with estimated diffusivity values) continues to be employed, and perhaps considered satisfactory. But, as this fails to explain the high activity of 10^5 g/g-cat h now attainable, the need for incorporating monomer convection in such a model is clear (McKenna et al., 1997; Weickert et al., 1999, Meier et al., 2001, McKenna and Soares, 2001, Kittilsen and McKenna, 2001). McKenna and Schweich (1992), McKenna et al. (1995), and Kittilsen et al. (2001) have approached the issue of convective flux as defined by the product of the superficial convective velocity (u) and the monomer concentration. But lacking the details of the calculation of u, we are unable to judge the nature of convection considered by them. Yiagopoulos et al. (2001) explicitly considered monomer diffusion through the pores in an expression for overall effective diffusivity, and defined convective transport by considering u to be the local particle expansion velocity. Thus, they considered convective transport of the monomer absorbed in the swollen polymer phase, but ignored the monomer convection through the pores.

In the subsection on the PFM with frozen boundary we present the governing equations of the PFM. The transformation of the moving-boundary problem into the fixed-boundary problem is then carried out as per Galvan and Tirrell (1986), incorporating the corrections of Byrne (1993). In the subsection on the MGM and its new solution, we present our extension of the PFM to simultaneously follow the growth of microparticles as in the framework of the MGM. As we shall see, this amounts to a significant computational simplification of the detailed MGM. In the subsection on the two-phase model, we supplement this model with an additional mode of monomer transport into the polymer particle, that is, monomer convection through the interconnected pores.

Both the PFM and the MGM models consider that the catalyst instantaneously breaks up into fragments. The fragmentation process *during* the polymerization has been modeled (Ferrero and Chiovetta, 1987; Przybyla et al., 1999b; Estenoz and Chiovetta, 2001), but we retain the assumption of instantaneous fragmentation to maintain simplicity. We restrict our consideration to homopolymerization, absence of inerts or diluents in the system, spherical catalyst particle, and only a single type of active site.

Theory

Polymeric flow model with frozen boundary

The diffusion-reaction processes in the growing polymer particle [$r < R(t)$] are described by the following balance equations:

Monomer diffusion and consumption by reaction

$$\frac{\partial M}{\partial t} = \frac{1}{r^2}\frac{\partial}{\partial r}\left(Dr^2\frac{\partial M}{\partial r}\right) - k_p AM \tag{1}$$

Flow and production of polymer

$$0 = \frac{\rho}{r^2}\frac{\partial}{\partial r}(ur^2) - k_p AM \tag{2}$$

Flow of catalyst sites with the polymer

$$\frac{\partial A}{\partial t} = -\frac{1}{r^2}\frac{\partial}{\partial r}(uAr^2) \tag{3}$$

The boundary conditions are

$$M = M_m \quad \text{at} \quad r = R \tag{4a}$$

$$\frac{\partial M}{\partial r} = 0 \quad \text{and} \quad u = 0 \quad \text{at} \quad r = 0 \tag{4b}$$

The initial conditions are

$$R = R_o \quad \text{and} \quad A = A_o \quad \text{at} \quad t = 0 \tag{5}$$

where R_o is the radius of the initial catalyst particle containing active sites with concentration A_o. The initial monomer concentration can be taken as one of the following:

(i) $M = 0$, that is, no monomer present at $t = 0$;

(ii) $M = M_o$, that is, in equilibrium with the surrounding medium, but no reaction at $t < 0$;

(iii) $M(r) = M_{ss}(r)$, that is, a *steady-state* profile corresponding to Eq. 1.

The particle radius R grows at the rate of polymer velocity at the particle surface

$$\frac{dR(t)}{dt} = u \quad \text{at} \quad r = R \tag{6}$$

We assume that there is neither any change in the catalytic activity of active sites, nor complete deactivation of the catalyst sites. Then, the total amount of active sites is given by

$$A_I(t) = 4\pi \int_0^{R(t)} r^2 A \, dr \tag{7}$$

which should remain constant as the particle grows.

We define the following dimensionless variables [Galvan and Tirrell (1986), Byrne (1993)]:

$$\bar{M} = \frac{M}{M_m}, \qquad \bar{M}_m = \frac{M_m}{\rho}, \qquad x = \frac{r}{R(t)},$$

$$\bar{R} = \frac{R}{R_o}, \qquad \bar{u} = \frac{uR_o}{D}, \qquad \bar{A} = \frac{A}{A_o}, \qquad \tau = \frac{Dt}{R_o^2}$$

and the Thiele modulus, $\alpha = \sqrt{R_o^2 (k_p/D) A_o}$. We emphasize that $\bar{R}$ represents the particle growth factor (radial), and the definition of the radial position variable, x, amounts to compression of the scale resulting in *freezing* of the moving boundary $r = R(t)$ to $x = 1$.

The system of equations is now rewritten in the dimensionless form (Byrne, 1993) as

$$\frac{\partial \bar{M}}{\partial \tau} = \frac{x}{\bar{R}} \bar{u}(1) \frac{\partial \bar{M}}{\partial x} + \frac{1}{\bar{R}^2} \frac{1}{x^2} \frac{\partial}{\partial x} \left(x^2 \frac{\partial \bar{M}}{\partial x} \right) - \alpha^2 \bar{A} \bar{M} \tag{8}$$

$$0 = \frac{1}{x^2} \frac{\partial}{\partial x} (x^2 \bar{u}) - \alpha^2 \bar{A} \bar{M} \bar{M}_m \bar{R} \tag{9}$$

$$\frac{\partial \bar{A}}{\partial \tau} + \left(\frac{\bar{u}}{\bar{R}} - \frac{x}{\bar{R}} \bar{u}(1) \right) \frac{\partial \bar{A}}{\partial x} = -\alpha^2 \bar{A}^2 \bar{M} \bar{M}_m \tag{10}$$

$$\frac{\partial \bar{R}}{\partial \tau} = \bar{u}(1) \tag{11}$$

Initial conditions are,

$$\bar{R} = 1 \qquad \bar{A} = 1 \qquad \bar{M} = 1 \quad \text{(or 0 or } SS \text{ profile)}. \tag{12}$$

Boundary conditions are,

$$\bar{M} = 1 \quad \text{at} \quad x = 1 \tag{13a}$$

and

$$\frac{\partial \bar{M}}{\partial x} = 0 \quad \text{and} \quad \bar{u} = 0 \quad \text{at } x = 0 \tag{13b}$$

The dimensionless parameters of the system are α and $\bar{M}_m$. We note that Galvan and Tirrell (1986) and Yiagopoulos et al. (2001) missed the $[(x/\bar{R})\bar{u}(1)]$ term in Eqs. 8 and 10. The latter also considered the local velocity, u, to be directly proportional to the local polymerization rate, rather than describing it by Eq. 2.

Multigrain model and its new solution

The multigrain model in its simplest form (Floyd et al., 1987) accounts for the diffusion phenomena on two different scales, that is, the microparticle and the macroparticle scales. Using M and D to denote the monomer concentration and effective diffusivity in the macroparticle at radial position r, its balance equation is written as

$$\epsilon \frac{\partial M}{\partial t} = \frac{1}{r^2} \frac{\partial}{\partial r} \left(D r^2 \frac{\partial M}{\partial r} \right) - (1 - \epsilon) R_p \tag{14}$$

where ϵ is the porosity (assumed constant) in the particle and

$$R_p = k_p A M^* \tag{15}$$

is the reaction rate based on polymer volume in the microparticle at that location, M^* being the monomer concentration at the catalyst surface (radius S_o) in the microparticle (of radius S) at that location. Thus, $\bar{S} = S/S_o$ is the microparticle growth factor (radial), S_o and S being the microparticle radius at location r at time 0 and present time t, respectively. We also note that A refers to the active site concentration based on polymer volume. If A' is the active site concentration based on catalyst volume, then $A = A'/\bar{S}^3$. Thus, A decreases from initial value A_o with microparticle growth, while A' decreases from the same initial value A_o only if deactivation (Floyd et al., 1987) is present:

$$\frac{dA'}{dt} = -k_d (A')^2 \tag{16}$$

where the second-order deactivation rate constant is related to the catalyst half-time as

$$t_{1/2} = (k_d A_o)^{-1} \tag{17}$$

Using the QSSA presented in Hutchinson et al. (1992), M^* is easily obtained as

$$M^* = \frac{\eta^* M}{1 + \dfrac{S_o^2}{3D_\mu} \left(1 - \dfrac{S_o}{S} \right) k_p A'} \tag{18}$$

where $\eta^* M$ represents the monomer concentration at the microparticle surface, M being the monomer concentration

in the macroparticle at that location and η^* being the corresponding equilibrium constant for monomer absorption in the microparticle.

The reported method of numerical simulation of MGM involves consideration of the macroparticle as being made up of microparticles in concentric spherical shells, and then a shell-by-shell evaluation of the concentration profiles (Floyd et al., 1987, Hutchinson et al., 1992). Further, since boundaries of these shells move with particle growth, a grid initialization and update procedure is required to follow the boundaries. Instead, we incorporate the important aspect of the MGM (that is, two scales of phenomena) in the following modification of the PFM, thereby eliminating the need to follow such a grid initialization and update. The displacement of microparticles is now presented as a continuous velocity (u) of the polymer in the porous particle, so that

$$0 = \frac{1}{r^2}\frac{\partial}{\partial r}\left[(1-\epsilon)ur^2\right] - \frac{(1-\epsilon)R_p}{\rho} \tag{19}$$

and

$$\frac{dR(t)}{dt} = u(R,t) \tag{20}$$

Here, the particle porosity, ϵ, has been taken as a constant, as in the early MGM (Floyd et al., 1987). Not only can the material displacement be followed in terms of differential equations, but also the microparticle growth can be described by the following equation:

$$\frac{\partial S}{\partial t} + u\frac{\partial S}{\partial r} = \frac{S}{3}\frac{R_p}{\rho} \tag{21}$$

The governing equations can now be modified as in the PFM case, by normalization of the radial variable as $x = r/R(t)$:

$$\epsilon\left[\frac{\partial M}{\partial t} - \frac{x}{R}u(1)\frac{\partial M}{\partial x}\right] = \frac{1}{R^2x^2}\frac{\partial}{\partial x}\left(Dx^2\frac{\partial M}{\partial x}\right) - (1-\epsilon)R_p \tag{22}$$

$$0 = \frac{1}{Rx^2}\frac{\partial}{\partial x}(ux^2) - \frac{R_p}{\rho} \tag{23}$$

$$\frac{\partial S}{\partial t} + \left[\frac{u}{R} - \frac{x}{R}u(1)\right]\frac{\partial S}{\partial x} = \frac{S}{3}\frac{R_p}{\rho} \tag{24}$$

$$\frac{dR(t)}{dt} = u(1,t) \tag{25}$$

The overall time-dependent reaction rate (g /g-cat time) can be calculated as

$$R_{\text{overall}} = 3\left(\frac{R}{R_o}\right)^3\frac{\rho M_w}{\rho_{\text{cat}}}\frac{d(R/R_o)}{dt} \tag{26}$$

where M_w is the molecular weight of the monomer. In the absence of diffusional limitations, its maximum possible value can be obtained from the catalyst's intrinsic reactivity as:

$$R_{\max} = k_p A_o M_m M_w/\rho_{\text{cat}} \tag{27}$$

Two-phase model

It is now well recognized (Keii et al., 1982; Ferrero et al., 1993; McKenna et al., 1999; Oleshko et al., 2001; Pater et al., 2001) that the growing polymer particle is indeed porous and that both diffusion and convection of the monomer make up the monomer transport within a growing particle. Yet, the existing models just mentioned consider only a diffusion contribution to monomer transport, but use an effective diffusion coefficient to account for transport through pores in the macroparticle. This is restrictive in the realistic two-phase situation because the transport mechanisms are essentially different, since the Fickian diffusion and convection flux are proportional to the gradients ($\partial M/\partial r$) and [$M(\partial P/\partial r)$], respectively. Further, while the pressure-driven convection through the pores would strongly depend on the pore size (which increases with particle growth), the effective diffusion coefficient was not considered to change during particle growth. Floyd et al. (1986) justified ignoring convective transport by arguing the convective transport is substantial primarily for homopolymerization cases involving no inerts or transfer agents. However, even in the presence of inerts, the phenomena like inerts enrichment cannot be described by the pure-diffusion model, as the monomer diffusion is driven by its own concentration gradient. Besides, with the newer and faster catalysts, the importance of incorporating the monomer's convective transport has increased (Weickert et al., 1999; McKenna and Soares, 2001).

We consider that the growing polymer particle is made up of spherical microparticles, with the interstitial spaces providing the pores through which monomer transport occurs by diffusion and convection. The convective transport of the undiluted monomer is driven by the pressure gradient created by the monomer consumption within the particle:

$$\epsilon\frac{\partial M}{\partial t} = \frac{1}{r^2}\frac{\partial}{\partial r}\left(r^2D\frac{\partial M}{\partial r} + \frac{1}{\mu_g}B_O r^2 M\frac{\partial P}{\partial r}\right) - (1-\epsilon)R_p \tag{28}$$

where the flow resistance in the pores is described by Darcy's law (Adler, 1998), the corresponding Darcy's coefficient

$$B_o = K_D\frac{\epsilon}{8\tau'}S^2 \quad K_D \sim 1 \tag{29}$$

being dependent on the porosity (ϵ), tortuosity (τ'), and the pore radius. Weickert et al. (1999) reported measuring the final pore diameter to be the same as the final microparticle diameter, and comparable growth factors for pore and macroparticle diameters. Based on this, we assume the pores to be the interstitial spaces between the microparticles, and the pore radius to be the same as the microparticle radius (S). Even though we realize this is not always the case, we make this assumption in the absence of a better description of pore-size variation during particle growth. For example,

McKenna et al. (1999) reported that large interconnected pores on the order of several microns were generated during slurry polymerization of ethylene. The role of such pore morphology in facilitating monomer convection to even larger extent is clear.

Limiting our consideration now to gas phase polymerization, and assuming that the gaseous monomer behaves as an ideal gas with concentration $M = P/R_gT$, the previous expression can be rewritten as

$$\epsilon\frac{\partial M}{\partial t} = \frac{1}{r^2}\frac{\partial}{\partial r}\left(\left(D + \frac{K_D R_g T}{\mu_g}\frac{\in}{8\tau'}S^2 M\right) r^2 \frac{\partial M}{\partial r}\right) - (1-\epsilon)R_p \quad (30)$$

Normalizing r with respect to $R(t)$, Eq. 30 is rewritten as

$$\epsilon\left[\frac{\partial M}{\partial t} - \frac{x}{R}u(1)\frac{\partial M}{\partial x}\right] = \frac{1}{R^2x^2}\frac{\partial}{\partial x} \times \left\{\left[1+\beta(S/S_o)^2(M/M_m)\right]x^2\frac{\partial M}{\partial x}\right\} - (1-\epsilon)R_p \quad (31)$$

where it is clear that the dimensionless number

$$\beta = \frac{K_D R_g T}{\mu_g D}\frac{\in}{8\tau'}S_o^2 M_m$$

is an indicator of the convection contribution as compared to diffusion. Thus, the convenience of incorporating the convection contribution in this two-phase model is largely based on the development carried out in the earlier sections, as the equations in the subsection on the MGM and its new solution (other than the monomer balance, Eqs. 14 and 22) remain directly applicable here.

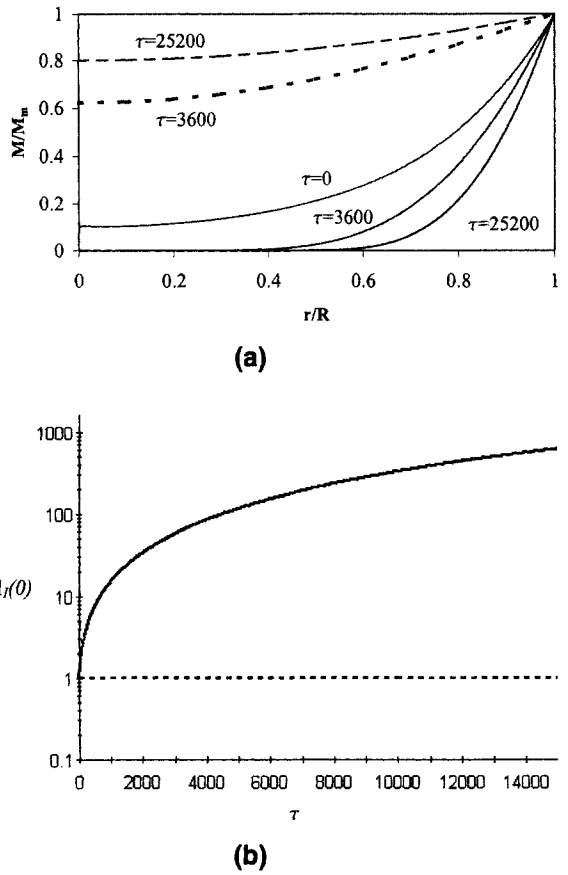

Figure 1. PFM (Eqs. 7–13) prediction of the development for $\alpha^2 = 20$, $M_m = 0.009$: (a) monomer concentration profiles; (b) total catalyst amount.

Results without (solid lines) and with (dashed lines) the $(x/\bar{R})u(1)$ correction terms are included. At $\tau = 0$, the initial concentration profile is the initial steady-state solution, and is the same for both cases.

Results and Discussion

PFM model

In this work, we have used gPROMS (General Process Modelling Systems) software with orthogonal collocated finite-element method (OCFEM) for solving systems of differential equations. We begin by verifying this tool by comparing our results with previous publications. The system of Eqs. 7–13 is solved without the $(x/\bar{R})u(1)$ term in Eqs. 8 and 10, and the results are shown as solid lines in Figure 1a for $\alpha^2 = 20$, $\bar{M}_m = 0.009$, which are the parameter values also used by Galvan and Tirrell (1986). Comparison of these solid lines in our Figure 1a with the curves in Figure 2 of Galvan and Tirrell (1986) shows an exact match (except that Galvan and Tirrell seem to have termed 3600 dimensionless time units as 1 h). This verifies that we have correctly implemented the numerical simulation tool. We then use Eq. 7 in the same simulation to calculate the total number of active catalyst sites (A_I) in the particle. The results, plotted in Figure 1b as a solid line, show that the model predicts the amount of catalyst to increase with particle growth. This is not possible physically, and the error is due to ignoring the $(x/\bar{R})u(1)$ term, which amounts to an incorrect mathematical attempt to freeze the moving boundary. Simulations were then carried out with the $(x/\bar{R})u(1)$ term as incorporated in Eqs. 8 and 10, and the results are included in Figure 1 as dashed lines for comparison with the situation when the $(x/\bar{R})u(1)$ term was ignored (solid lines). When the $(x/\bar{R})u(1)$ term is included, the amount of catalyst in the particle remains constant (Figure 1b), thus removing the inconsistency. Further, the concentration profiles begin to approach $\bar{M} = 1$ (Figure 1a, dashed lines), suggesting elimination of diffusional limitations right from the beginning, in contrast to Galvan and Tirrell's prediction (solid lines) of depleting concentrations, that is, increasing diffusional limitations at an early stage.

MGM model

The MGM is solved using the sets of equations, Eqs. 15–18 and 22–25, for the parameter values listed in Table 1, as also employed by Floyd et al. (1987) for slurry-phase polymerization of propylene. The results presented in Figure 2a show a good match with Figure 4 of Floyd et al. (1987). This suggests the MGM can indeed be simulated by the system of equa-

Table 1. Parameters for Simulation of Slurry Polymerization of Propylene (Figure 2)

Parameter	Value
k_p (L/mol·s)	24,600
M_m (mol/L)	4
η^*	1
$t_{1/2}$ (h)	0.25
D_μ (cm^2/s)	10^{-8}
D (cm^2/s)	10^{-5}
ρ (mol/cm^3)	0.0238
ρ_{cat} (g/cm^3)	2.84
ϵ	0.3
R_o (μm)	15
S_o (μm)	0.5
A_o(mol/g-cat)	1×10^{-5}

tions (Eqs. 15–18 and 22–25). The advantages of such a system and solution technique for MGM as compared to the method employed earlier in the literature are that one no longer needs a shell-by-shell and grid update procedure. Polymer flow in the macroparticle (that is, displacement of microparticles) is now presented as a continuous variable $u(r,t)$, the velocity of the polymer in the porous particle. Equation 24 allows us to follow the microparticle growth as well, and the results at some radial locations in the growing particle are presented in Figure 2b. As can be clearly seen, the microparticle growth is fast at the polymer-particle surface ($x = 1$) right at the beginning. At the center of the polymer particle ($x = 0$), the initial microparticle growth rate is smaller due to diffusional limitations, but increases within the first seconds to the same level as that of the microparticles at the surface of the polymer particle.

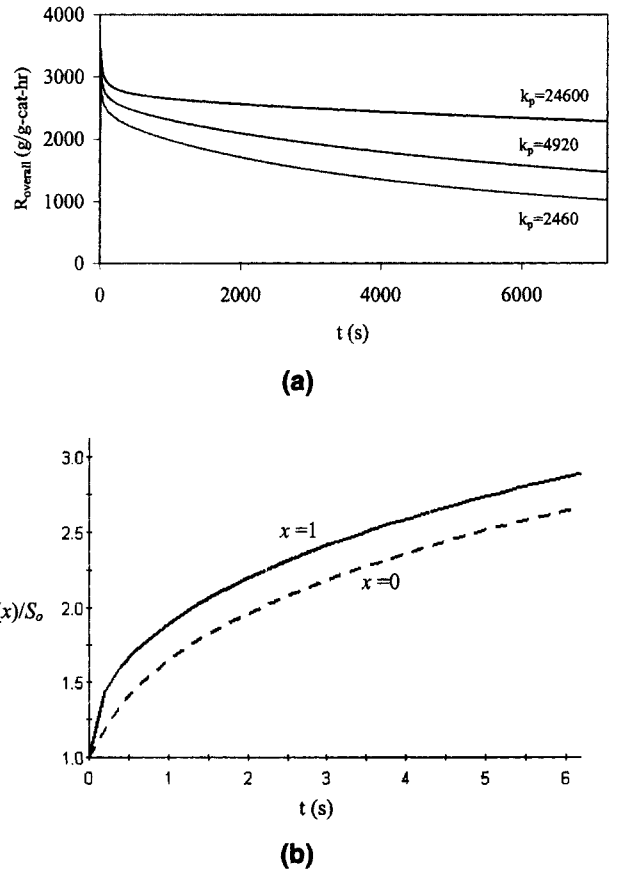

Figure 2. MGM (Eqs. 15–18, 22–25) predictions for the slurry-phase propylene polymerization for parameter values in Table 1.

(a) Reaction rate, and (b) microparticle growth factors at particle center ($x = 0$) and particle surface ($x = 1$).

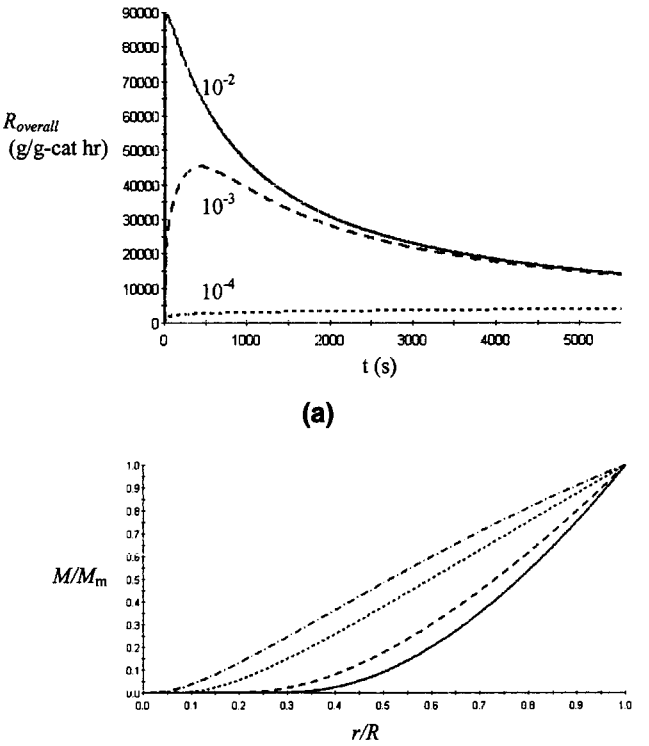

Figure 3. MGM predictions for gas-phase propylene polymerization for parameter values in Table 2.

(a) Reaction rate for different macroparticle-level diffusivities (D, cm^2/s) shown in the figure, and (b) monomer concentration profiles for $D = 10^{-4}$ cm^2/s, at different times (t = 20, 100, 1000, and 5000 s, higher curves at higher time).

Weickert et al. (1999) reported polymerization rates of 0.8 $\times 10^5$ g/g-cat h for gas and liquid pool polymerization of propylene. Kittilsen and McKenna (2001) recently observed peak catalytic activity of 10^5 g/g-cat h during ethylene polymerization following slower prepolymerization steps. This goes to say that the intrinsic catalytic activity of modern catalysts can indeed be so high. Meier et al. (2001) recently reported activities of 10^5 g/g-cat h for gas-phase propylene polymerization. Using the estimated parameter values from their experiments, as listed in Table 2, and ignoring the microparticle diffusion resistance (i.e., $M^* = M$), we carried out the MGM simulations (subsection on the MGM and its new solution). The results presented in Figure 3a for various values of macroparticle diffusivity indicate that diffusional limitations are eliminated and that the intrinsic reactivity predicted *only if* the macroparticle diffusivity is higher than 10^{-2} cm^2/s. Although the value of monomer diffusivity is somewhat uncertain, and a recent discussion on this topic can be

Table 2. Parameters for Simulation of Gas-Phase Polymerization of Propylene (Figures 3–4)

Parameter	Value
$k_p A_o$ (s)	1878*
M_m (mol/L)	1
η^*	1
$t_{1/2}$ (h)	0.25
D_μ (cm^2/s)	∞
D (cm^2/s)	10^{-4}
ρ (mol/cm^3)	0.0238
ρ_{cat} (g/cm^3)	2.84
ϵ	0.3
τ'	6
R_o (μm)	108
S_o (μm)	0.2
T (K)	343

*From Eq. 27, using $R_{max} = 10^5$ g/g h.

found in Yiangopoulos et al. (2001), the effective diffusivity is of the order ($D \sim 10^{-3}$–10^{-4} cm^2/s). MGM simulations (Figure 3a) predict serious diffusional limitations at such diffusivities. As seen from the monomer concentration profiles in Figure 3b, the monomer depletion and the extent of diffusional limitations are predicted to decrease with the progress of the reaction, but rather slowly. Significant diffusion limitations are predicted even at 5000 s after the start of the reaction.

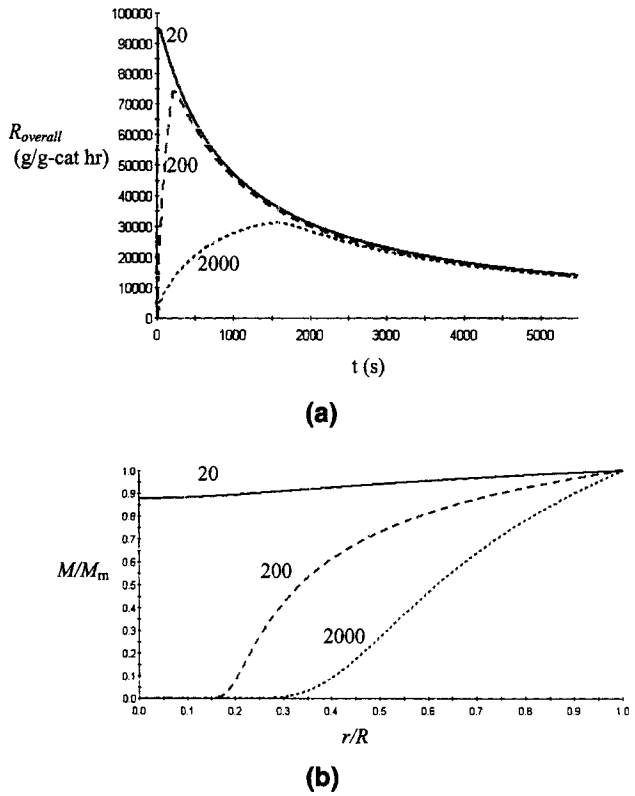

Figure 4. Two-phase model predictions for gas-phase propylene polymerization for parameter values in Table 2, and μ_g (cP) values in the figures: (a) reaction rate and (b) monomer concentration profiles at $t = 20$ s.

Two-phase model

For the same set of parameters as used in Figure 3 and the convection parameters listed in Table 2, we carried out simulations of the two-phase model by solving Eqs. 15–18, 23–26, and 31. The results for various values of the gas viscosity (μ_g) are presented in Figure 4a. We note that, at μ_g values of 20 cP or lower, reaction rates close to the intrinsic value $R_{max} = 10^5$ g/g-cat h are quickly achieved, before decreasing due to catalyst deactivation. The absence of mass-transfer limitations at $\mu_g = 20$ cP or lower is also seen from the monomer concentration being close to the maximum at all radial positions (Figure 4b). We can thus conclude that at the practical viscosities values of about 0.2 cP, convection will provide sufficient monomer transport, and macroparticle mass transfer will not be rate-limiting, at least for the present case of undiluted gaseous monomer. We also note that, while the profiles in Figure 3b correspond to a parabolic differential equation, the deviation, in the shape of the monomer concentration profiles of Figure 4b, is related to the nonlinear nature of their governing Eq. 31.

Conclusions

The MGM is very often used to examine the role of diffusional limitations in the olefin polymerization rate on heterogeneous catalysts. In the past, its simulation has involved determination of monomer concentration profiles sequentially for each radial shell of microparticles, with both boundaries of the radial shells moving with the particle growth. We have presented a fixed boundary system of simultaneous differential equations that enables easier computer implementation of the simplest form of the MGM.

In addition to simplifying the analysis of the MGM, we have extended it to a two-phase model that directly accounts for the monomer transport by convection through the interstitial pores between the growing microparticles. Such monomer transport is driven by the pressure gradient created by monomer consumption. While both PFM and MGM predict significant diffusional resistance at the high activities obtained with modern catalysts, we find the monomer convection through pores contributes substantially to the total monomer transport in gas-phase polymerization. From a simple analysis of the reported high activity propylene polymerization experiment, it appears that at practical viscosity values of less than 0.2 cP, convection provides sufficient monomer transport for intrinsic reaction rates to be achieved, at least for the case of undiluted gaseous monomer. The presence of inert solvents in the reaction medium may reduce the convection contribution due to inerts accumulation in the pores, and are being examined (Parasu Veera et al., 2001).

It is desirable to incorporate much of the last three decades of advancements of MGM into the solution methodology presented in this article. Some such issues that remain to be considered include the morphology determining microparticle movement, porosity variation, copolymerization, molecular-weight distributions, catalyst distribution and decay, mul-

tiple active sites, and external mass-transfer resistance. Further, it is important to consider the heat-transfer effects, because the rapid generation of the heat and its insufficient removal can lead to temperature gradients in the particle (McKenna et al., 1999; Yiagopoulos et al., 2001), and the accompanying variations in the monomer diffusivity and viscosity, the M-P relationship, among others. It is also important to point out that the method of freezing the moving boundary, enabling a simpler mathematical representation, that is presented here, can provide alternatives to the techniques used for analysis of other situations. Examples of such processes are the pressure- or diffusion-induced growth/collapse of spherical bubbles (Agarwal, 2002); the swelling and dissolution of polymer particles, such as during controlled drug release; polymer processing operations like blow molding; microparticle growth during olefin polymerization; and drug encapsulation by interfacial polymerization.

Notation

A = catalyst concentration (based on volume of polymer particle), kmol·m^{-3}
A' = catalyst concentration (based on catalyst volume), kmol·m^{-3}
A_o = initial catalyst concentration, kmol·m^{-3}
$\bar{A}$ = dimensionless catalyst concentration
B_o = Darcy's coefficient
D = diffusion coefficient at the macroparticle level, m^2·s^{-1}
D_μ = diffusion coefficient at the microparticle level, m^2·s^{-1}
k_p = propagation rate constant, m^3·kmol^{-1}·s^{-1}
k_d = deactivation rate constant, m^3·kmol^{-1}·s^{-1}
K_D = a constant in Darcy's equation, ~1
M = monomer concentration, kmol·m^{-3}
M_m = maximum monomer concentration, that is, at particle surface, kmol·m^{-3}
$\bar{M}$ = dimensionless monomer concentration, M/M_m
$\bar{M}_m$ = fractional concentration of monomer, M_m/ρ
M_w = molecular weight of the monomer, kg·kg mol^{-1}
P = monomer pressure, Pa
P_{ext} = monomer pressure in the reaction medium containing the growing particle, Pa
r = radial location in the growing particle
R_g = universal gas constant, N·m·kmol^{-1}·K^{-1}
R_p = rate of reaction, based on polymer volume, kmol·m^{-3}·s^{-1}
$R_{overall}$ = overall rate of reaction, kg·kg-cat^{-1}·s^{-1}
R_o = initial radius of the particle, m
R = radius of the particle at time t, m
$\bar{R}$ = (macro)particle growth factor
S = radius of the micro particle, m
S_o = initial microparticle radius, m
$\bar{S}_o$ = dimensionless initial microparticle radius
$\bar{S}$ = dimensionless microparticle radius
t = time, s
$t_{1/2}$ = half-life of the catalyst, s
T = temperature, K
u = velocity of the swollen polymer, m·s^{-1}
$\bar{u}$ = dimensionless velocity of swollen polymer
x = dimensionless radial position

Greek letters

α = Thiele modulus in the PFM case
β = dimensionless number
ϵ = porosity
η^* = monomer sorption coefficient
τ = dimensionless time
τ' = tortuosity
μ_g = monomer viscosity, Pa·s
ρ = density of monomer or monomer swollen polymer, kmol·m^{-3}
ρ_{cat} = density of catalyst, kg·m^{-3}

Literature Cited

Adler, P. M., *Porous Media, Geometry and Transports*, Butterworths-Heinemann, London (1992).

Agarwal, U. S., "Modeling Olefin Polymerization on Heterogeneous Catalyst: Polymer Resistance at Microparticle Level," *Chem. Eng. Sci.*, **53**(23), 3941 (1998).

Agarwal, U. S., "Simulation of Bubble Growth and Collapse in Linear and Pom-Pom Polymers," *e-Polymers*, 14 (2002).

Byrne, G. D., "The Taming of Copolymerization Model with VODE," *IMPACT Comput. Sci. Eng.*, **5**, 318 (1993).

Estenoz, D. A., and M. G. Chiovetta, "Olefin Polymerization Using Supported Metallocene Catalysts: Process Representation Scheme and Mathematical Model," *J. Appl. Poly. Sci.*, **81**, 285 (2001).

Ferrero, M. A., R. Sommer, P. Spanne, K. W. Jones, and W.C. Conner, "X-ray Microtomography Studies of Nascent Polyolefin Particles Polymerized over Magnesium Chloride-Supported Catalyst," *J. Poly. Sci.*, **31**, 2507 (1993).

Ferrero, M. A., and M. G. Chiovetta, "Catalyst Fragmentation During Propylene Polymerization: Part I. The Effect of Grain Size and Structure," *Poly. Eng. Sci.*, **27**, 1436 (1987).

Floyd S., K. Y. Choi, T. W. Taylor, G. E. Mann, and W. H. Ray, "Polymerization Olefins Through Heterogeneous Catalysts: III. Particle Modelling with an Analysis of Intraparticle Heat and Mass Transfer Effects," *J. Appl. Poly. Sci.*, **32**, 2935 (1986).

Floyd, S., T. Heiskanen, T. W. Taylor, G. E. Mann, and W. H. Ray, "Polymerization Olefins Through Heterogeneous Catalysts. VI. Effect of Particle Heat and Mass Transfer on Polymerization Behaviour and Polymer Particles," *J. Appl. Poly. Sci.*, **33**, 1021 (1987).

Galvan, R., and M. Tirrell, "Orthogonal Collocation Applied to Analysis of Heterogeneous Ziegler-Natta Polymerization," *Comput. Chem. Eng.*, **10**, 77 (1986).

Hoel, E. L., C. Cozewith, and G. D. Byrne, "Effect of Diffusion on Heterogeneous Ethylene Propylene Copolymerization," *AIChE J.*, **40**, 1669 (1994).

Hutchinson, R. A., C. M. Chen, and W. H. Ray, "Polymerization of Olefins Through Heterogeneous Catalysts X: Modelling of Particle Growth and Morphology," *J. Appl. Poly. Sci.*, **44**, 1389 (1992).

Keii, T., E. Suzuki, M. Tamura, M. Murata, and Y. Doi, "Propene Polymerization with a Magnesium Chloride-Supported Ziegler-Natta Catalyst-1: Principal Kinetics," *Macromol. Chem.*, **183**, 2285 (1982).

Kittilsen, P., and T. F. McKenna, "Study of the Kinetics, Mass Transfer, and Particle Morphology in the Production of High Impact Polypropylene," *J. Appl. Poly. Sci.*, **82**, 1047 (2001).

Kittilsen, P., H. Svendsen, and T. F. McKenna, "Modeling of Transfer Phenomena on Heterogeneous Ziegler Catalysts. IV. Convection Effects in Gas Phase Processes," *Chem. Eng. Sci.*, **56**, 3997 (2001).

McKenna T. F., D. Cokljat, R. Spitz, and B. Schweib, "Modelling of Heat and Mass Transfer During the Polymerization of Olefins on Heterogeneous Ziegler Catalysts," *Catal. Today*, **48**, 101 (1999)

McKenna, T. F., J. Dupuy, and R. Spitz, "Modelling of Transport Phenomena on Heterogeneous Ziegler Catalysts: Difference Between Theory and Experimental in Olefin Polymerization (An Introduction)," *J. Appl. Polym. Sci.*, **57**, 371 (1995).

McKenna T. F., J. Dupuy, and R. Spitz, "Modelling of Transport Phenomena on Heterogeneous Ziegler Catalysts: Modeling of Intraparticle Mass Transfer Resistance," *J. Appl. Polym. Sci.*, **63**, 315 (1997).

McKenna, T. F., and D. Schweich, "Modelling of Mass and Energy Transport During the Copolymerization of Ethylene and 1-Butene on Ziegler Catalysts: Models of Catalyst Particle Morphology and Transport Phenomena," K. H. Reichert and H. O. Moritz, eds., *Fourth Annual Workshop on Polymer Reaction Engineering* VCH, Berlin p. 169 (1992).

McKenna, T. F., and J. B. P. Soares, "Single Particle Modelling for Olefin Polymerization on Supported Catalysts: A Review and Proposals for Future Developments," *Chem. Eng. Sci.*, **56**, 3931 (2001).

Meier, G. B., G. Weickert, and W. P. M. van Swaaij, "Gas-Phase Polymerisation of Propylene: Reaction Kinetics and Molecular Weight Distribution," *J. Polym. Sci., Chem. Educ.*, **39**, 500 (2001).

Nagel, E. J., V. A. Krillov, and W. H. Ray, "Prediction of Molecular Weight Distributions for High Density Polyolefins," *Ind. Eng. Chem. Prod. Res. Dev.*, **19**, 372 (1986).

Naik, S. D., and W. H. Ray, "Particle Morphology for Polyolefins Synthesized with Supported Metallocene Catalysts," *J. Appl. Poly. Sci.*, **79**, 2565 (2001).

Oleshko, V. P., P. A. Crozier, R. D. Cantrall, and A. D. Westwood, "In-Situ and Ex-Situ Microscopic Study of Gas Phase Propylene Polymerization over a High Activity $TiCl_4$-$MgCl_2$ Heterogeneous Ziegler-Natta Catalyst," *Macromol. Rapid Commun.*, **22**, 34 (2001).

Parasu Veera, U., N. E. Benes, M. S. Pimplapure, W. P. M. van Swaaij, and G. Weickert, "Mass Transport During Olefin Polymerization on Heterogeneous Catalysts," *Int. Workshop on Polymer Reaction Engineering*, K. H. Reichert and H. U. Moritz, eds., Wiley-VCH, Frankfurt, p. 391 (2001).

Pater, J. T. M., G. Weickert, J. Loos, and W. P. M. van Swaiij, "High Precision Prepolymerization at Extremely Low Reaction Rates-Kinetics and Morphology," *Chem. Eng. Sci.*, **56**, 4107 (2001).

Przybyla, J., B. Zechlin, B. Seinmetz, B. Tesche, and G. Fink, "Influence of Particle Size on the Kinetics and the Resulting Polymer Properties at the Polypropylene Polymerization with Heterogeneous Metallocene Catalysts: Part 1: Experimental Studies and Kinetic Analysis," *Metal Organic Catalysis for Synthesis and Polymerization*, W. Kiminsky, ed., Springer-Verlag, Berlin, p. 321 (1999a).

Przybyla, J., B. Weimann, and G. Fink, "Influence of Particle Size on the Kinetics and the Resulting Polymer Properties at the Polypropylene Polymerization with Heterogeneous Metallocene Catalysts: Part 2: Development of Model as Well as Mathematical Simulation," *Metal Organic Catalysis for Synthesis and Polymerization*, Walter Kiminsky, eds., Springer-Verlag, Berlin, p. 333 (1999b).

Schmeal, W. R., and J. R. Street, "Polymerization in Expanding Catalyst Particles," *AIChE J.*, **17**, 1188 (1971).

Singh, D., and R. R. Merrill, "Molecular Weigh Distribution of Polyethylene Produced by Ziegler-Natta Catalysts," *Macromol.*, **4**, 599 (1971).

Weickert, G., G. B. Meier, J. T. M. Pater, and K. R. Westerterp, "The Particle as a Microreactor: Catalytic Propylene Polymerization with Supported Metallocene and Ziegler-Natta catalysis," *Chem. Eng. Sci.*, **54**, 3291 (1999).

Yermakov, Y. I., V. G. Mikhaichenko, V. S. Besco, Y. P. Grabovski, and I. V. Emirov, (Original in Russian) *Plast. Massy*, **9**, 7 (1970).

Yiagopoulos, A., H. Yiannoulakis, V. Dimos, and C. Kiparissides, "Heat and Mass Transfer Phenomena During the Early Growth of a Catalyst Particle in Gas-Phase Olefin Polymerization: The Effect of Prepolymerization Temperature and Time," *Chem. Eng. Sci.*, **56**, 3979 (2001).

Manuscript received Nov. 12, 2001, and revision received July 11, 2001.